Complex metallic alloys as new materials for additive manufacturing

Samuel Kenzari, David Bonina, Jean-Marie Dubois, Vincent Fournée

Science and Technology of Advanced Materials

ISSN: 1468-6996 (Print) 1878-5514 (Online) Journal homepage: http://www.tandfonline.com/loi/tsta20

Complex metallic alloys as new materials for additive manufacturing

Samuel Kenzari, David Bonina, Jean Marie Dubois & Vincent Fournée

To cite this article: Samuel Kenzari, David Bonina, Jean Marie Dubois & Vincent Fournée (2014) Complex metallic alloys as new materials for additive manufacturing, Science and Technology of Advanced Materials, 15:2, 024802, DOI: 10.1088/1468-6996/15/2/024802

To link to this article: http://dx.doi.org/10.1088/1468-6996/15/2/024802

OPEN ACCESS
IOP Publishing | National Institute for Materials Science
Science and Technology of Advanced Materials
Sci. Technol. Adv. Mater. **15** (2014) 024802 (9pp)
doi:10.1088/1468-6996/15/2/024802

Review

Complex metallic alloys as new materials for additive manufacturing

Samuel Kenzari, David Bonina, Jean Marie Dubois and Vincent Fournée

Institut Jean Lamour, UMR 7198 CNRS-Université de Lorraine, F-54011 Nancy, France

E-mail: vincent.fournee@univ-lorraine.fr

Received 28 January 2014
Accepted for publication 1 April 2014
Published 30 April 2014

Abstract

Additive manufacturing processes allow freeform fabrication of the physical representation of a three-dimensional computer-aided design (CAD) data model. This area has been expanding rapidly over the last 20 years. It includes several techniques such as selective laser sintering and stereolithography. The range of materials used today is quite restricted while there is a real demand for manufacturing lighter functional parts or parts with improved functional properties. In this article, we summarize recent work performed in this field, introducing new composite materials containing complex metallic alloys. These are mainly Al-based quasicrystalline alloys whose properties differ from those of conventional alloys. The use of these materials allows us to produce light-weight parts consisting of either metal–matrix composites or of polymer–matrix composites with improved properties. Functional parts using these alloys are now commercialized.

Keywords: quasicrystals, composites, additive manufacturing, tribology

1. Introduction

Additive manufacturing technologies were first used for rapid prototyping but are now increasingly being used to produce a series of end user functional parts. It consists in producing a three-dimensional (3D) object, usually layer by layer, from a single computer file (a CAD model). These technologies are opposed to more traditional subtractive methods, such as machining, which proceed by removal of material to obtain the 3D object. These new manufacturing methods are becoming widespread and affect a lot of industries (automotive, aerospace, machinery, medical and dental, design, etc). They generated global revenues of $2.204 billion in 2012 and the average annual growth over the 2010–2012 period was around 28% [1].

The selective laser sintering (SLS) is one such method developed and patented by Deckard *et al* [2]. The process used in this study operates as follows. The object is first modeled in a CAD file and decomposed into as many two-dimensional (2D) layers as necessary, with a thickness of the order of 100 μm. The layers are built successively according to the principle illustrated in figure 1. A first layer of powder is spread by an automated roll on a platform and an infrared laser is used to convert the powder to a solid object by 'selective sintering' without external pressure according to the 2D plot defined by the CAD model. The powder used contains at least one polymer whose melting temperature is generally about 200 °C. The powder bed is preheated a few degrees below its melting point and the laser just provides locally the thermal energy required to bring the polymer to its melting temperature. Un-melted powders naturally provide support for the following layers. Then the build platform is moved down by the thickness of one layer, a new layer of powder is spread onto the previous one and the cycle repeats itself to build the part from bottom to top.

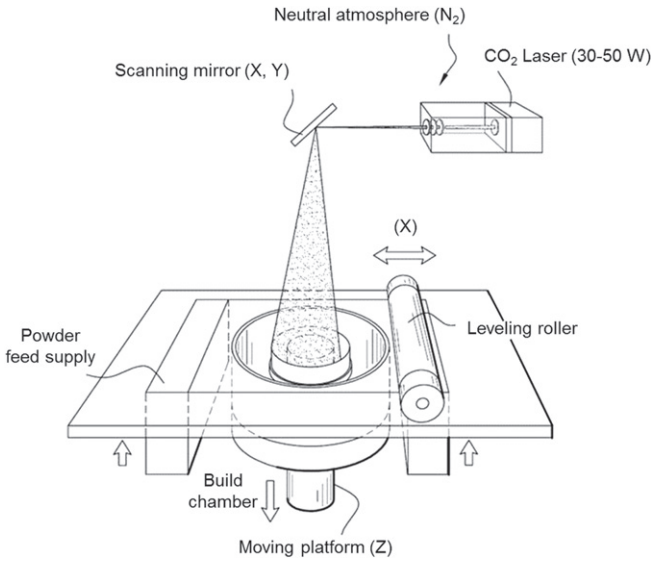

Figure 1. Schematic description of the SLS process used. The laser builds 2D section of the parts according to the CAD model. Then the platform is lowered and another layer of powder is spread onto the previous one. The process is repeated until the 3D part is completed. Un-melted powders serve as support for the next layers.

The SLS process is used to construct parts that are either entirely made of polymer or a polymer composite reinforced by different kinds of particles or even a metal matrix composite [3, 4]. The latter is referred to as indirect SLS because it requires a two-step process. First, a porous preform must be obtained by SLS of a powder mixture containing metal particles and a polymer binder. At this stage, the object is a metal/polymer composite containing 40–50% of pores by volume. It is rigid enough to be handled but has no sufficient mechanical strength to be used directly. In a second step, this preform is submitted to a heat treatment during which the polymer is debinded and simultaneously infiltrated by a filler metal whose melting point is necessarily lower than that of the metal used in the preform. Infiltration of the porous preform with the liquid filler metal occurs by capillarity. This two-step process leads to composite metal parts made entirely of the metal base and the filler metal. In practice, the indirect SLS is a well-controlled process only for steel/brass composites.

Since the year 2000s, a series of studies was conducted to extend the materials range for indirect SLS, and especially towards light alloys like aluminum alloys [5]. Today, these developments are still at the stage of being a technological challenge. Aluminum is also used in direct SLS, incorporated into a polymer matrix to obtain composite parts with a metallic appearance [6]. Basically, SLS polymer composites have a high level of porosity which prohibits their direct use in applications requiring a perfect seal at low thicknesses of parts without post-impregnation of resin. This sealing problem exists also for all other reinforcing materials used in direct SLS, not just aluminum. To circumvent this problem, reinforced polymer composite parts must undergo a second processing step of impregnation with a liquid resin to fill the porosity. In addition, the friction and wear properties of composite parts produced by direct SLS are relatively poor, which limits their use for movable parts.

The work presented in this article shows how some of the problems mentioned above could be solved through the introduction of complex metallic alloys (CMAs) as new materials for rapid manufacturing technologies. In the case of indirect SLS, it is possible to obtain fully functional metal parts made of different light alloys (Al-based). In the case of direct SLS, CMA particles are used as reinforcement particles in a polymer matrix to improve the properties of composite parts. CMA particles can also be used as reinforcement particles in resin composites made by stereolithography (SL).

2. CMAs

CMAs are defined as intermetallic compounds with large unit cells, containing several tens up to several thousands of atoms. Inside the unit cell, atoms usually form geometrical cluster units of high symmetry, for example icosahedral (five-fold symmetry) or decagonal (ten-fold symmetry) clusters. These clusters are interconnected by so-called glue atoms to develop a 3D structure. There has been a renewed interest in such complex compounds since the discovery of quasicrystals (QCs) by Dan Shechtman in 1982 [7]. QCs can be viewed as the ultimate degree of complexity in CMAs, with a unit cell of infinite dimension and the loss of the translational invariance characterizing conventional crystals. QCs first attracted attention due to their unique atomic structure, inducing a paradigm shift in crystallography. In parallel, intriguing physical properties were reported, not expected for intermetallic compounds (for a recent review, see [8]). Among them, the thermal and electronic transport properties were found to be non-metallic in several systems like Al–Cu–Fe QCs, although they are made of metals.

From the point of view of technological applications, CMAs have often been presented as promising new materials because of their potentially useful properties like low coefficients of friction, relatively good corrosion resistance, low wettability, good wear resistance, etc [9]. Such functional properties are however difficult to implement due to the intrinsic brittleness of CMAs which prevents their use as bulk materials. Two main alternatives have been considered to circumvent this problem. One is to use these phases as reinforcement particles in a ductile matrix like Al-based [10, 11] or a polymer matrix [12]. The other is to use CMAs as new coating materials [9, 13].

In the following sections, we will summarize and discuss the use of CMAs in metal matrix or polymer matrix composites processed by additive manufacturing technologies. The properties of resulting parts will also be described and compared to existing state of the art industrial solutions [14–18].

Figure 2. Left: picture of a porous preform made by SLS containing Al–Cu–Fe–B QC particles and a polymer binder. The lateral dimension of the preform is 5 cm. Right: SEM image of the mixed powder after selective sintering showing the formation of polymer bridges connecting the QC particles.

3. Manufacturing of metallic parts by indirect SLS

The indirect SLS method is currently well controlled for steel/brass composites but the density of this composite (8 g cm^{-3}) is much too high for many applications. Therefore many studies have been conducted in order to extend this process to produce light-weight Al-based composites. First, a porous preform containing particles of a preliminary Al alloy of a certain grade and a polymer binder must be produced by SLS. Then the porous preform has to be infiltrated with a liquid Al alloy of a different grade characterized by a lower melting point than the Al alloy used in the preform. All attempts to produce such Al-based composites by indirect SLS have led to parts presenting poor mechanical strength [6, 19]. The origin of this brittleness is due to the nitriding of the interfaces during the debinding process, which according to [19] is a necessary step to achieve complete infiltration of the preform and maintain its dimensional accuracy.

This problem can be circumvented by manufacturing a preform based on CMA particles and a polymer binder, which can then be infiltrated with a commercial Al alloy. One key advantage of Al-based CMAs is their thermal stability (larger than 800 °C for Al–Cu–Fe–B QC for example) which is far above any commercial Al grade while still possessing low density (< 4.7 g cm^{-3}). First a suitable powder mixture is prepared by blending Al–Cu–Fe–B QC particles with polyamide (PA) (Nylon) particles. The polymer represents approximately 2.5% in weight of the total blend. The QC particles are produced by gas atomization. They have a nominal composition of $Al_{59}Cu_{25.5}Fe_{12.5}B_3$ (at.%) and contain primarily the quasicrystalline phase together with a small amount of the β-$Al_{50-x}(Cu,Fe)_{50+x}$ phase. This powder mixture is used to prepare a preform by SLS, an example being shown in figure 2. Typically, such a preform contains about 40% volume fraction of open porosity. Analysis of the microstructure by scanning electron microscopy (SEM) reveals that the PA particles are melted by the laser during SLS and form bridges between the QC particles (figure 2). The preforms are brittle at this stage but can be easily manipulated. Infiltration is realized in a pre-evacuated furnace ($1{\cdot}10^{-2}$ mbar) back-filled with an inert atmosphere. The preform is placed in a crucible on a sacrificial tab together with blocks of the infiltrating metal (figure 3). In this, an Al 1050 grade was used, i.e. a commercial Al alloy having a melting point of around 660 °C. The crucible is then filled with alumina particles in order to support the preform during the debinding and infiltration process. The crucible is heated up to the melting of the infiltrant (3 h, 680 °C), which can then fill in the open porosity of the preform by capillarity.

Figure 3 shows an example of a preform successfully infiltrated by a 1050 Al alloy. The nitriding step was not necessary in order to keep the dimensionality of the part and achieve complete infiltration. The parts contain little porosity as seen in the SEM image in figure 3, achieving values similar to those observed for steel–brass composite parts. X-ray diffraction analysis reveals that the parts are composed of several CMA phases and do not contain crystalline aluminum anymore. The absence of fcc aluminum in the final composite results from phase transformations induced by chemical diffusion of Al into the CMA particles during the infiltration cycle. The QC phase mainly transforms into tetragonal ω-$Al_{70}Cu_{20}Fe_{10}$, an alloy known for its beneficial contribution in Al matrix composites due to the improvement of the bonding strength between the Al matrix and the particles [20, 21]. The composite parts exhibit high hardness values (in the range of Vickers hardness 300–400 Hv), which is remarkable for Al-based materials but which makes them fragile. However it is possible to optimize the process by applying post-infiltration heat treatments and reduce the hardness down to about 200 Hv. These values are similar to those of steel/brass parts, but the final density of the QC-Al1050 composites is lower by a factor of 2, which was the targeted objective.

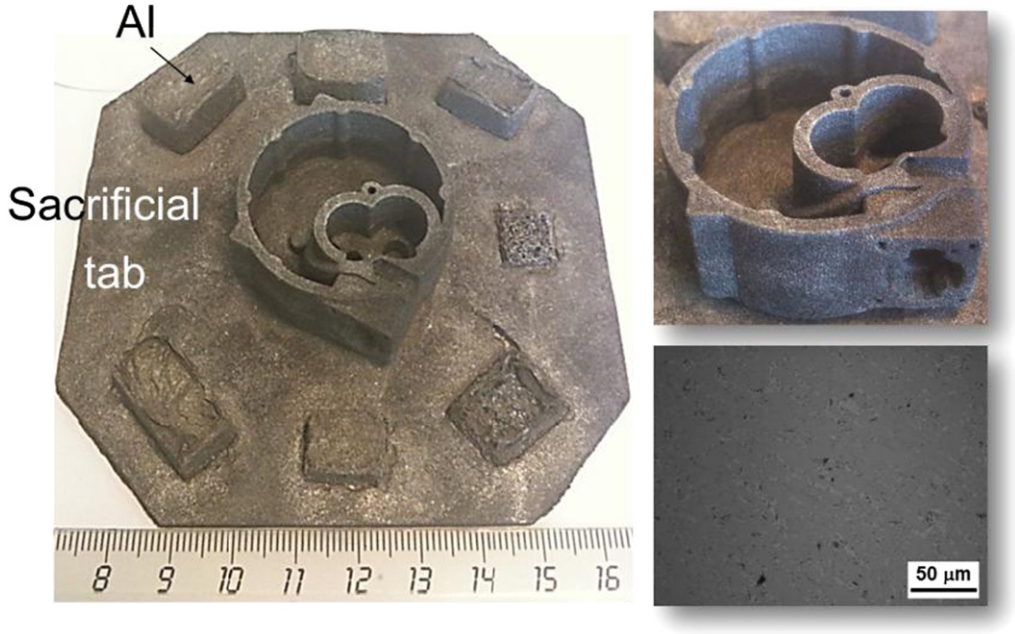

Figure 3. Left: picture of the infiltrated preform placed on the sacrificial tab surrounded by a block of Al infiltrant. Right: the top part shows a picture of infiltrated preform. The part is now fully metallic and contains several CMA phases but no fcc Al. The bottom part shows an optical image of the infiltrated preform indicating a low level of porosity.

The bottleneck to achieve a successful technology transfer of the process relies on the ability to precisely control the thermal cycle during the infiltration in industrial conditions. It is important that the thermal treatment is applied for sufficient time to complete infiltration as well as chemical diffusion at the interfaces. However, if the infiltration temperature is too high or if the holding time is too long, then the parts may start to deform. The high melting point of Al-based QC particles is thus clearly an advantage compared to commercial Al grades because the temperature window for the infiltration of the filler metal is much larger.

To conclude this section, a new range of composite powders based on CMAs was developed to produce all-metal parts of any complex shape by indirect SLS technology [16]. The composite parts are entirely metallic; they contain a low level of porosity and have a low mass density. This method can in principle be extended to a broad spectrum of chemical compositions by varying the nature of the selected CMA phase.

4. Manufacturing of CMA-polymer composite parts by direct SLS

Earlier works by Bloom *et al* have shown that QC used as reinforcement particles in a polymer matrix lead to composite materials with improved wear resistance and reduced friction [22, 23]. In this section, we show that such QC-polymer composites can be adapted to SLS technology to manufacture functional 3D composite parts. The polymer matrix is made of PA 12 (Nylon) with a low density ($<1.5\,g\,cm^{-3}$) and is reinforced by Al–Cu–Fe–B QC particles obtained by gas atomization representing more than 50 wt.% of the total blend [17]. The QC particles were sieved with a mesh size of 75 μm and blended with nylon particles ($<75\,\mu$m) in a Turbula mixer (30 min) in the appropriate volume fraction (30 vol.% of QC) optimized for the laser sintering process. Selective laser sintered parts were then constructed using a sPro™ 60 SLS® Center. The parameters used in SLS (laser, temperature, scanning speed, etc) have been optimized to yield dense parts, unconstrained shape, dimensional accuracy and a quality of skin similar to those of commercial composite parts normally produced by SLS. They are given in table 1. The maximum size (*xyz*) of the parts which can be produced in this experimental setup can reach $380\times330\times450$ mm (≈60 l). An example is shown in figure 4. The friction, wear and sealing properties of the composite material have been studied and compared to other PA matrix composites. The main results are summarized below.

4.1. Friction properties

Friction tests were carried out at room temperature in ambient atmosphere with a relative humidity of 50–60% and under non-lubricated conditions. The indenter was a 6 mm ball of 100Cr6 hard steel. The radius of the trace was 5 mm. The sliding velocity was $15\,cm\,s^{-1}$ (300 rpm) and the normal load was 10 N. The sample surfaces were first mechanically polished using SiC paper in water lubricant (from 500 grit down to 4000 grit) and cleaned with methanol and dried. The ratio between the lateral force measured using a pin-on-disk tribometer and the applied normal force gives the friction coefficient μ.

The friction curves measured on a series of composite samples prepared by SLS are shown in figure 5. The samples are PA matrix composites reinforced by either

Figure 4. Picture of an intake manifold made of a polyamide composite reinforced by QC particles. This part is used in automotive industry and is produced by SLS in a single processing step. The size of the component is about $20 \times 30 \times 40$ cm. Reproduced from [14], Copyright (2012), with permission from Elsevier.

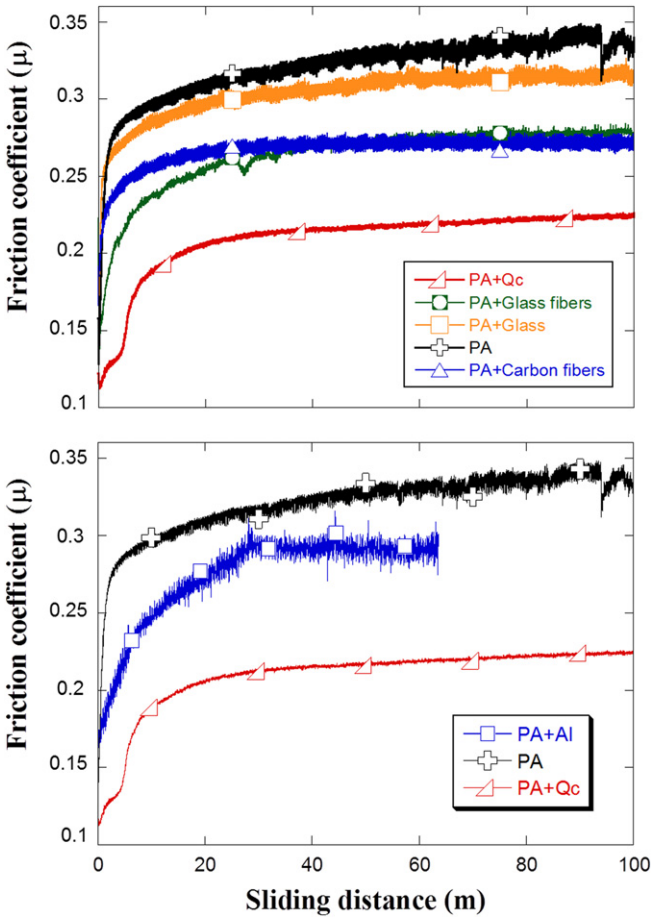

Figure 5. Top and bottom: friction coefficients measured as a function of the sliding distance for PA composites filled with various reinforcement particles or fibers. Adapted from [14], Copyright (2012), with permission from Elsevier.

commercial fillers (carbon fibers, glass fibers, glass particles) or Al–Cu–Fe–B QC particles. The results clearly show that the lowest friction coefficients are obtained for composites reinforced by the QC particles. Other PA composites reinforced by Al particles of similar size and volume fraction than the QC particles were also tested. In this later case, all friction tests were stopped after about 65 m of sliding distance due to strong tangential forces (figure 5). SEM investigations of the worn surface (figure 6) and indenter (figure 7) show that the wear track and the ball counterpart are covered by a transferred layer which is made up primarily of aluminum and oxygen. When QCs are used as filler particles, no material transfer occurs and the surface of the composite is hardly degraded when the friction test ends.

4.2. Wear tests

Wear resistance of SLS samples was evaluated under lubricating water conditions using a standard polishing technique (SiC paper, 500 grit, normal load 10 N, 1 min, 150 rpm). Figure 8 compares the wear volumes measured for different composites produced by SLS or by hot pressing (180 °C, 5 min, 15 MPa). The QC filler particles provide the best wear resistance compared to all other types investigated, with a gain of up to 70% compared to unfilled PA or PA–Al composite. The comparison between SLS and hot-pressed samples shows similar properties, indicating that the composites are not affected by the SLS process compared to other conventional polymer manufacturing technologies.

4.3. Sealing properties

Surprisingly, and in contrast to conventional SLS composites, the relative density of the composite parts reinforced by QC particles is close to 99% of the theoretical density. This value only reaches 85% for composite reinforced by Al particles. This very low porosity makes the PA–QC composites directly leak tight under air or water pressure (up to 7 bars) and for operating temperatures larger than 100 °C. This sealing property is only met for PA–QC composites. For all other commercial composite powders with similar particle size and volume fraction, an additional step of post-impregnation of the parts with a resin is necessary in order to fill the residual porosities and make the parts leak tight. This additional step increases the manufacturing time of the parts by approximately a factor of 2. Therefore the sealing property of PA–QC parts is a great advantage for many fluidic applications. The functional part in figure 4 is one such example. It shows an intake manifold of a car engine with wall thickness of only 2 mm. The fact that the new composite material is directly leak tight allows to one fabricate this part in one single operation, whereas using conventional materials, one would have to first build the parts in two halves by SLS, then process with resin impregnation and finally bond the two halves together. Other examples already on the market include hoses, inserts, adaptors, connectors, etc used in automotive engineering but other niche applications emerge as well like domestic appliances.

Table 1. Experimental parameters used to construct SLS parts.

Laser conditions				Temperatures (°C)			Feed parameter
Power (W)	Beam diameter (mm)	Scan speed (mm s^{-1})	Scan fill spacing (mm)	Bed	Feed	Piston	Layer thickness (mm)
48	0.42	12 100	0.22	173	140	150	0.1

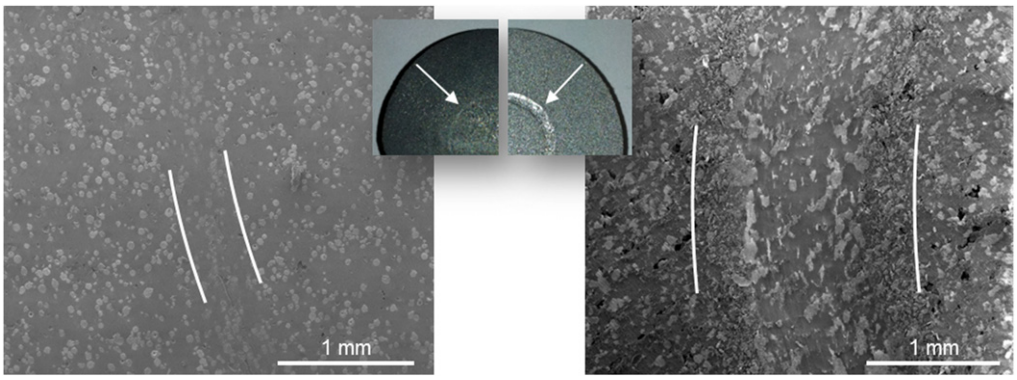

Figure 6. SEM images of the worn surfaces of the PA composites reinforced by QC particles (left) and Al particles (right) observed after ending the friction test. Insets are optical micrographs of the sample showing the wear tracks. Adapted from [14], Copyright (2012), with permission from Elsevier.

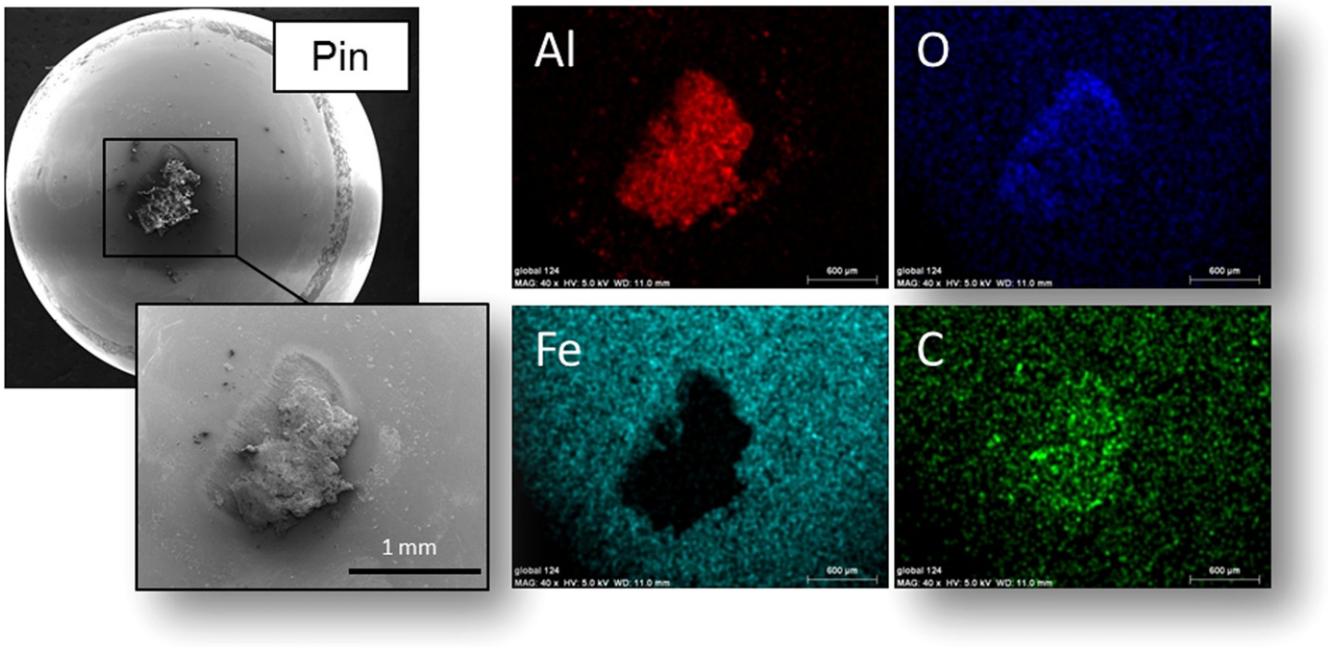

Figure 7. Left: SEM images of the 100Cr6 pin after sliding on the PA–Al composite indicating material transfer from the sample to the pin. Right: chemical maps of the pin obtained by wavelength-dispersive x-ray spectroscopy.

The origin of this sealing property must relate to some specific properties of the QC particles compared to other filler materials. One hypothesis could be that the wetting properties of the melted polymer are better on QC particles, allowing for reduced residual porosity of the SLS parts. We have tested this hypothesis by measuring contact angles formed by liquid polymer droplets deposited on a bulk sample of either the QC phase or a pure Al sample prepared by sintering. However, a good wettability (contact angle lower than 90°) is found in both cases. Another hypothesis would be that the effect of the laser beam during the sintering process is more effective in melting the PA powders in the presence of QC particles compared to Al particles, such that the polymer binder remains liquid for a longer time upon beam exposure thus leaving less porosity. As mentioned earlier in the introduction, the powder bed in SLS is pre-heated at a temperature

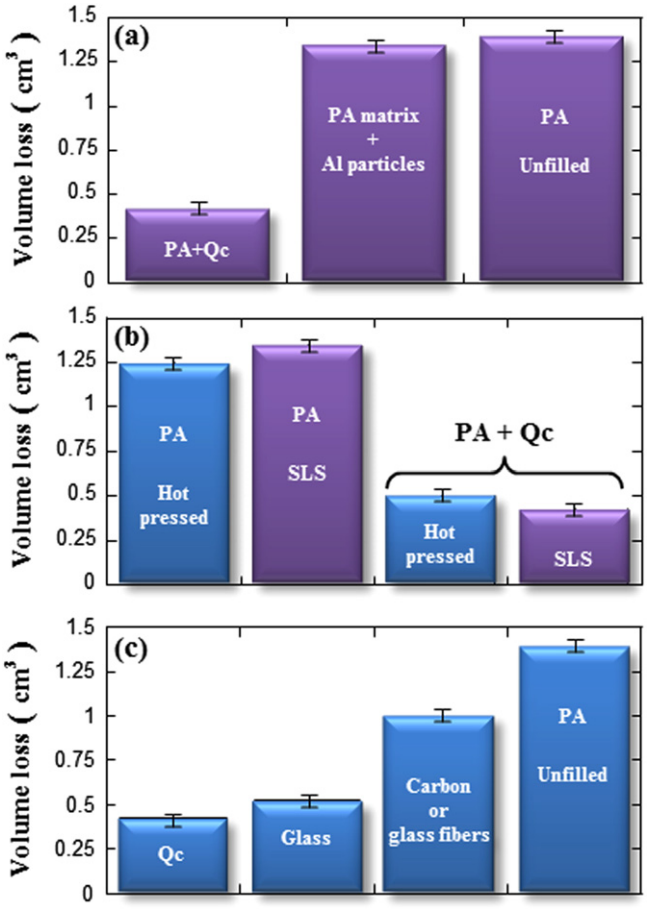

Figure 8. (a) Volume loss for SLS samples. When aluminum particles are added to the PA matrix, no gain is observed compared to unfilled PA. Quasicrystalline particles (QCs) reduce the volume loss by about 70%. (b) Volume loss results of hot pressed samples compared to SLS samples. (c) Comparison of SLS composites reinforced by QC particles with commercial SLS samples filled by glass particles, carbon fibers and glass fibers. Adapted from [14], Copyright (2012), with permission from Elsevier.

that is just a few degrees below the melting point of the polymer binder and the laser beam only provides locally the additional energy required to melt the binder. The optical properties of QCs are known to differ significantly from normal metals like Al, absorbing more efficiently the IR light of the CO_2 laser beam. Therefore one expects that the embedded QC particles will adsorb more efficiently the laser beam energy, leading to a larger temperature increase and more effective melting of the surrounding polymer. In addition, the thermal conductivity of Al–Cu–Fe–B QC is about one hundred times lower than that of Al, a property which should further contribute to a more effective melting upon beam exposure.

5. Quasicrystal-resin composites for stereolithography

SL is another additive manufacturing technology [24]. Its principle is similar to the SLS technology in the sense that it is also used to build 3D objects layer-by-layer. The main difference is that it uses a UV laser beam to polymerize locally a liquid resin monomer according to the 2D pattern of the CAD model, whereas SLS uses an IR laser to melt locally the polymer binder. Physically, the solidification consists in a photo-initiated polymerization, linking monomers into larger molecules by free radical reaction upon laser exposure. The resin must be solidified to a depth that must be larger than the layer thickness such that one layer adheres to the previous one. Once a layer has been completed, the part support is lowered into the vat containing the liquid resin by one layer thickness. The thin layer of liquid resin is then solidified (polymerized) according to the next 2D section and the process is repeated until the 3D part is completed, from bottom to top. The SL technology is widely used for both prototyping and manufacturing of functional parts for end users. However one disadvantage of this method compared to other rapid fabrication technologies is the limited range of available materials. The photo-curable resin can be filled with ceramic powders, and also glass or carbon fibers. Composites reinforced by metal particles have not been developed except for very small particle size, making its cost prohibitive for practical applications. The technological bottleneck is that filler particles added to the resin act as scattering centers for the incident light beam because of partial reflection and diffusion at the particle surfaces, limiting the penetration depth of the UV beam and thus the layer thickness.

Here again, the optical properties of QCs have been decisive in circumventing this problem and a QC–resin mixture could be successfully developed to build 3D functional parts by SL. The photo-curable resin is a commercial epoxy (Accura Si40®, 3D Systems). It contains cycloaliphatic epoxy resin (30–60 wt.%), aliphatic polyolpolyglycidyl (5–20 wt.%) and photoinitiators (0.1–10 wt.%) and has a density of 1.1 g cm^{-3}. The same Al–Cu–Fe–B QC particles produced by gas atomization were used as reinforcement particles. They were sieved with a mesh size of 25 μm. The optical reflectivity of the QC powders has been measured in the UV–visible range and compared to that of Al raw powders with similar particle size distribution. It was found that the reflectivity of the QC powder is much lower than that of Al at the wavelength of the UV laser used in SL (UV Nd–YAG laser, 355 nm wavelength).

The resin and the QC particles were mixed using a planetary mill with ceramic balls for 40 min at 100 rpm and ball-to-mixture weight ratio of 2:1. The optical reflectivity of the resin mixed with 20% volume of QC particles has been measured and compared to unfilled resin or resin mixed with 20% volume of Al particles as well as to a commercial resin filled with nanosized ceramic particles named Bluestone [25] (figure 9). The reflectivity is below 5% at the wavelength of the UV laser for the unfilled resin, the commercial Bluestone resin and the QC–resin mixture. It becomes much larger (15%) when Al particles are used, indicating that the photopolymerization of the mixture will be less efficient in this case. The polymerization depth of the QC–resin mixture was measured as a function of the density of energy provided by the laser and for different volume fraction of the filler

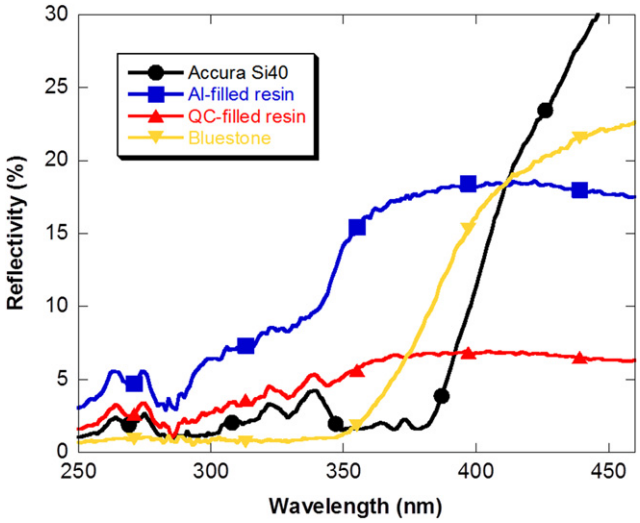

Figure 9. Reflectivity measurements in the UV–visible region of the different samples surfaces. Adapted from [15], Copyright (2014), with permission from Elsevier.

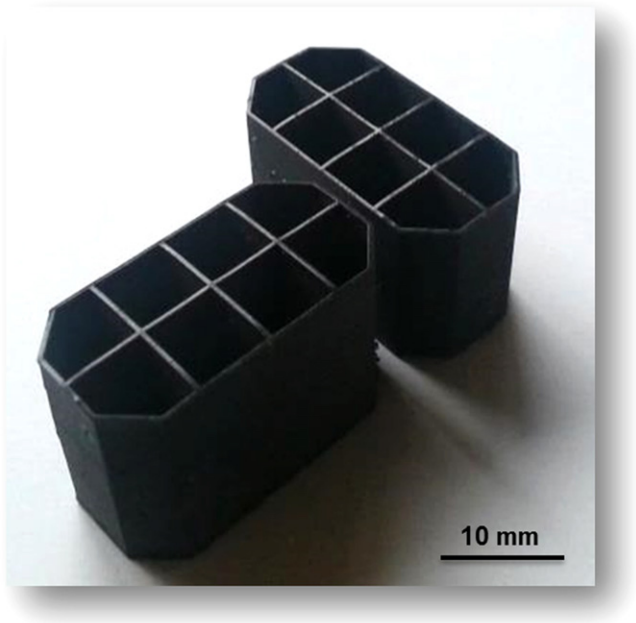

Figure 10. Picture of QC–resin composite parts produced by stereolithography. Adapted from [15], Copyright (2014), with permission from Elsevier.

particles. The largest polymerization depth (70 μm) was obtained for a mixture containing 20% volume of QC particles and a laser energy density of 2 J m^{-2}. These values are compatible with the fabrication of 3D objects by adding up layers of about 50 μm in thickness, thus providing sufficient overlap between two consecutive layers. Note that under similar experimental conditions, the polymerization depth measured for the same resin filled with 20% volume of Al particles was lower than 30 μm, making it impossible to consider such composite for manufacturing by SL. Therefore the unusual optical properties of QC materials compared to normal metals [26] are a definite advantage when considering these materials as filler particles in SL resins.

An example of such QC–resin 3D parts obtained by SL is shown in figure 10. Cross-sections of the parts have been investigated by optical microscopy revealing a homogeneous distribution of the QC particles, both within a layer and in the direction perpendicular to the layers. A linear shrinkage of the parts is typically observed in SL, due to the volume change of the polymer resin upon solidification. For a 25 mm diameter cylinder made of unfilled resin, the linear shrinkage is estimated to about 1.9% and is reduced to ~1.3% for the commercial Bluestone resin and to ~1% for the QC filled resin (20% vol.), allowing for improved manufacturing precision.

Finally, friction and wear behavior of QC–resin composite parts have been tested and compared to that of the unfilled resin as well as of the Bluestone resin which presents the best performance available on SL market. The Shore D hardness of the QC–resin composites (87.5 ± 1) is found to be intermediate between the unfilled resin (83 ± 1) and the Bluestone resin (92 ± 1). The wear resistance was evaluated under lubricating water conditions using a standard polishing technique (SiC paper, 500 grit, normal load 10 N, 30 s, 150 rpm). The wear losses are reduced by ~40% in the case of QC filled resin compared to the unfilled resin, close to the value observed for the Bluestone

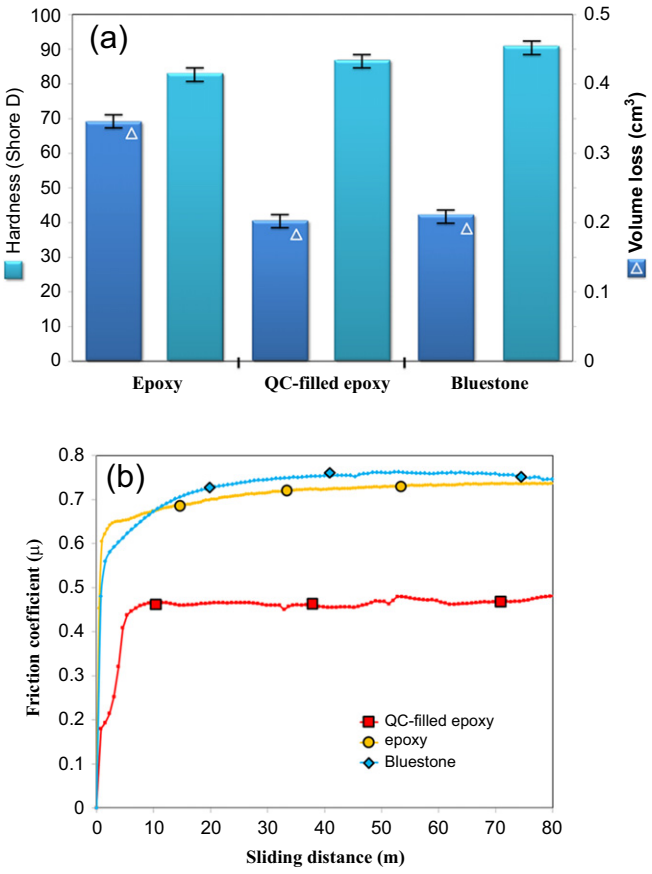

Figure 11. (a) Shore D hardness values (left scale) and abrasive volume loss (right scale) measured for the pure resin, the QC–resin composite and the commercial Bluestone resin. (b) Friction coefficients as a function of the sliding distance measured for the same samples. Adapted from [15], Copyright (2014), with permission from Elsevier.

nanocomposites (figure 11). The friction coefficients were measured using a pin-on-disk tribometer at room temperature in ambient atmosphere with a relative humidity of 50–60% and under non-lubricated conditions. The indenter was a 6 mm ball of 100Cr6 hard steel. The radius of the trace was 5 mm. The sliding velocity was 7.85 cm s^{-1} (150 rpm) and the normal load was 5 N. The results are shown in figure 11 as a function of the sliding distance. The friction coefficients show the same behavior for the unfilled resin and the Bluestone, with a value of ∼0.7. The friction coefficient becomes unstable in the case of the unfilled resin after 80 m of sliding distance as a result of material damage in the contact area. The friction forces are reduced by ∼30% in the case of the QC filled resin and remain stable. These results are similar to those reported in section 4.1 for PA matrix reinforced by QC particles made by SLS. In addition, a pronounced abrasion of the 100Cr6 pin was observed by SEM after the friction test on the Bluestone composite and chemical maps revealed some material transfer from the composite sample to the pin. This is due to the presence of silica nanoparticles in the Bluestone resin which are known as strongly abrasive. Some material transfer was also observed from the QC–resin composite to the pin (presence of aluminum oxide on the pin) but no significant abrasion was reported in this case. Therefore the QC–resin composite for SL manufacturing might prove useful for industrial applications requiring good mechanical properties and reduced friction coefficients [15, 18].

6. Conclusions

The field of additive manufacturing technologies is growing rapidly and concerns many industrial sectors such as automotive, aerospace, tooling, medical and dental, design, etc. These technologies are conceptually similar to 3D printing and are not limited to polymer materials. They allow the manufacture of series of parts with more and more demanding functional properties and therefore the development of new materials adapted to these technologies is important.

In this article, we have demonstrated that CMAs such as QCs can be useful to design new composite materials adapted to additive manufacturing technologies. Light-weight metal–matrix composites have been developed to build 3D parts having mechanical properties similar to those of steel–brass composites used currently in the industry but having a density lower by a factor of 2. Polymer matrix composites reinforced by QC particles have been developed for both the direct SLS and SL technologies. These composites present several advantages in comparison to other materials currently available on the market and some of them are now commercialized [17, 27].

Acknowledgments

This work was supported by the National Centre for Scientific Research (CNRS), the Region Lorraine and Ateliers CINI SA.

References

[1] Wohlers T 2013 *Wohlers Report, Additive Manufacturing and 3D Printing State of the Industry* (Colorado: Wohlers Associates)
[2] Deckard C, Beaman J J and Darrah J 1988 *Patent Cooperation Treaty Application* WO 9208567
[3] Kruth J P, Vandenbroucke B, Van Vaerenbergh J and Mercelis P 2005 *Proc. 1st Int. Conf. on Polymers and Moulds Innovations (Belgium)* p 525
[4] Stewart T D, Dalgarno K W and Childs T H C 1999 *Mater. Des.* **20** 133
[5] Sercombe T B and Schaffer G B 2003 *Science* **301** 1225
[6] Mazzoli A, Moriconi G and Pauri M G 2007 *Mater. Des.* **28** 993
[7] Shechtman D, Blech I, Gratias D and Cahn J W 1984 *Phys. Rev. Lett.* **53** 1951
[8] Dubois J M 2012 *Chem. Soc. Rev.* **41** 6760
[9] Dubois J M, Kang S S and Massiani Y 1993 *J. Non-Cryst. Solids* **153-154** 443
[10] Tsai A P, Aoki K, Inoue A and Masumoto T 1993 *J. Mater. Res.* **8** 5
[11] Inoue A and Kimura H 2000 *Mater. Sci. Eng.* A **286** 1
[12] Bloom P D, Baikerikar K G, Otaigbe J U and Sheares V V 2000 *Mater. Sci. Eng.* A **294-296** 156
[13] Sordelet D J, Besser M F and Logsdon J L 1998 *Mater. Sci. Eng.* A **255** 54
[14] Kenzari S, Bonina D, Dubois J M and Fournée V 2012 *Mater. Des.* **35** 691
[15] Sakly A, Kenzari S, Bonina D, Corbel S and Fournée V 2014 *Mater. Des.* **56** 280
[16] Kenzari S and Fournée V 2008 *French Patent* FR *2929541* (2009 *Patent Cooperation Treaty Application* WO2009/144405)
[17] Kenzari S and Fournée V 2009 *French Patent* FR *2950826* (2011 *Patent Cooperation Treaty Application* WO2011/039469)
[18] Sakly A, Kenzari S, Bonina D, Corbel S and Fournée V 2012 *French Patent* FR *2990375* (2013 *Patent Cooperation Treaty Application* WO2013/167448)
[19] Sercombe T B and Schaffer G B 2004 *Acta Mat.* **52** 3019
[20] Lee S M, Jung J H, Fleury E, Kim W T and Kim D H 2000 *Mat. Sci. Eng.* A **294-296** 99
[21] Tang F, Anderson I E and Biner S B 2003 *Mat. Sci. Eng.* A **363** 20
[22] Sheares V V and Bloom P D 2000 *Patent Cooperation Treaty Application* WO2000/056538
[23] Bloom P D, Baikerikar K G, Anderegg J W and Sheares V V 2001 **643** K1631–12
[24] André J C, Le Mehaute A and De Witte O 1984 *French Patent* FR 8411241
[25] 3D Systems Accura® Bluestone material datasheet (www.3dsystems.com, accessed April 2014)
[26] Demange V, Milandri A, de Weerd M C, Machizaud F, Geandel G and Dubois J M 2002 *Phys. Rev.* B **65** 144205
[27] Kenzari S and Fournée V 2011 *French Patent* FR *2979269* (2013 *Patent Cooperation Treaty Application* WO 2013/026972)